Oxygen-induced reconstructions of Cu(110) studied by reflectance difference spectroscopy

L. D. Sun, M. Hohage, and P. Zeppenfeld*
Institut für Experimentalphysik, Johannes Kepler Universität Linz, A-4040 Linz, Austria
(Received 9 July 2003; published 15 January 2004)

The optical anisotropy of the oxygen-induced (2×1) and $c(6\times2)$ reconstructions on Cu(110) corresponding to oxygen coverages of 1/2 and 2/3, respectively, has been studied by reflectance difference spectroscopy (RDS). The oxygen derived RDS features have been characterized and found to depend linearly on the oxygen coverage in the range between $\Theta=1/2$ and $\Theta=2/3$. This allows the quantitative, real-time monitoring of the $c(6\times2)$O$\rightarrow(2\times1)$O phase transition induced upon annealing to temperatures above 660 K.

DOI: 10.1103/PhysRevB.69.045407 PACS number(s): 78.40.−q, 68.35.Bs, 68.43.−h, 78.68.+m

I. INTRODUCTION

Oxygen adsorption on Cu(110) leads to a pronounced restructuring of the surface.[1] Depending on the oxygen coverage Θ, two well ordered superstructures may be obtained upon oxygen adsorption on the Cu(110) surface: a (2×1)O phase with $\Theta=1/2$ and a $c(6\times2)$ phase when Θ reaches 2/3.[1] Numerous experimental and theoretical studies have dealt with the oxygen-induced (2×1) reconstruction during the last decades, which lead to a deep understanding of the atomic and electronic structures as well as the ''added-row'' growth mechanism. In contrast, investigations of the oxygen-induced $c(6\times2)$ reconstruction are much more scarce, albeit its important role as a further step towards bulk oxidation. A structure model that involves an oxygen coverage $\Theta=2/3$ has been derived from a combined scanning tunnel microscopy (STM), x-ray diffraction, and effective-medium theory (EMT) study[2] and has been confirmed by low-energy electron-diffraction (LEED) *I-V* analysis.[3] Two different recipes have been used to create this high oxygen density reconstruction, namely, a high-temperature and a low-temperature adsorption process. At elevated surface temperature ($T_s\geqslant300$ K), a $c(6\times2)$ structure is only fully developed after an oxygen exposure of about 10^6 L (1 L $=10^{-6}$ torr s),[1] whereas at low temperature (83 K), an oxygen exposure as low as 1.9 L followed by annealing above room temperature is enough to form a $c(6\times2)$ structure with an oxygen coverage of 2/3.[4,5] The fact that such a low oxygen exposure is sufficient to form the $c(6\times2)$ phase at low temperature has been explained by the presence of oxygen in the molecular state which dissociates later during annealing.[4] This argument is supported by a low-temperature STM study of Briner *et al.*[6] and molecular-beam experiments of Hodgson *et al.*[7] The former visualized the trapping of weakly bound, physisorbed oxygen molecules and the latter reveals the increase of the initial sticking probability of oxygen molecules at temperatures below 100 K. Finally, the fully developed $c(6\times2)$O phase is stable up to temperatures of 610 K; further annealing above this temperature leads to a reduction of the oxygen surface coverage and a concomitant phase transition of $c(6\times2)\rightarrow c(6\times2)+(2\times1)\rightarrow(2\times1)$. The decrease of the oxygen surface coverage was suggested to be due to oxygen diffusion into the Cu bulk.[5]

In the present contribution, we report a study on the optical anisotropy of the Cu(110)-$c(6\times2)$O surface with an oxygen coverage of 2/3 prepared at low temperature, together with a quantitative investigation by reflectance difference spectroscopy (RDS) of the $c(6\times2)\rightarrow(2\times1)$ phase transition at elevated temperature. Finally, a real-time RDS study was performed to characterize the kinetics of this phase transition.

II. EXPERIMENT

All the experiments reported here have been carried out in an UHV chamber equipped with facilities for auger electron spectroscopy (AES), LEED, STM, and temperature programmed desorption. The residual gas pressure is below 10^{-10} mbar. A high-quality single-crystal Cu(110) sample with a miscut angle $<0.1°$ has been used in this study. The sample is mounted on a manipulator and can be cooled to 10 K by means of a continuous flow liquid He cryostat, to which the sample holder is connected via a copper braid. Using an electron impact heater fixed at the backside, the sample can be heated to above 1000 K. A programmable temperature control unit allows the sample temperature to be set and hold at any intermediate temperature, and the heating and cooling rate can be controlled accurately. The sample temperature is measured with a *K*-type thermocouple clamped to the crystal. The temperature reading has been calibrated at low temperature by thermal desorption of several kinds of gases, and the error is estimated to be smaller than ±1 K. The Cu(110) surface is cleaned by sputtering with 900 eV Ar^+ ions at room temperature and subsequent annealing to 800 K. After the preparation, the surface impurity is lower than the detection limit of AES; and the LEED image reveals a sharp $p(1\times1)$ diffraction pattern.

The main experimental method involved in this study is RDS, which measures the difference of the normal-incidence reflectivity for two mutually perpendicular orientations of the polarization vector as a function of the photon energy.[8,9] For cubic crystals, the optical response from the bulk is isotropic and the RDS signal arises only from the surface induced optical anisotropy. This makes RDS a highly surface sensitive optical probe, providing information on the surface structure, morphology, and electronic properties. The technique is widely used in the study of semiconductor surfaces and their growth in various environments. More recently, RDS has also been applied to metal surfaces such as

Cu(110),[10–12] Ag(110),[13–15] and Au(110).[16,17] It has been demonstrated that RDS is extremely sensitive to adsorption,[18,10] surface structural changes during sputtering,[19] and surface reconstruction.[17]

The RDS spectrometer used in the present study is of the Aspnes type[20] and is attached to the chamber via a strain-free optical window. The light from a Xe lamp is directed on the sample at normal incidence with the polarization axis oriented at an angle of 45° with respect to the two main crystalline axes $[1\bar{1}0]$ and $[001]$ of the Cu(110) surface. The change of the polarization state of the reflected light is measured using the modulation/lock-in technique. With the use of a monochromator, the reflected light is further analyzed with respect to the photon energy. As a result, the normalized reflectance difference defined as

$$\frac{\Delta r}{r} = \frac{2(r_{[1\bar{1}0]} - r_{[001]})}{r_{[1\bar{1}0]} + r_{[001]}} \tag{1}$$

can be recorded as a function of the photon energy in a range between 1.5 eV and 5.5 eV. To avoid any temperature effects on the RDS signal, all RDS spectra in this paper have been recorded at the same sample temperature of 11 K.

III. RESULTS AND DISCUSSION

A. The Cu(110)-$c(6\times2)$O phase and its optical anisotropy

In the current experiments, the sample is cooled down to 11 K after preparation. The real part of the RDS spectrum obtained from the clean Cu(110) surface at 11 K is shown in Fig. 1(a). The most pronounced peak at 2.1 eV contains two contributions, namely, a transition between an occupied and an unoccupied surface state located at the $\bar{Y}$ symmetry point of the surface Brillouin zone and a surface modified bulk transition related to the onset of the interband transitions ($\Delta_5 \rightarrow \Delta_1$) in copper occurring in the vicinity of the bulk symmetry point X.[11,12] The small peak at 4.1 eV is due to the transition between an occupied surface resonance to an unoccupied surface state at $\bar{X}$ of the surface Brillouin zone. The negative peak at 4.3 eV and the positive peak at 5 eV originate from surface modified bulk transitions in the vicinity of high symmetry point L ($E_F \rightarrow L_1^u$ and $L_2' \rightarrow L_1^u$), respectively.[21]

Figure 1(b) shows the real part of the RDS spectrum after adsorption of 1 L of oxygen on the Cu(110) surface at 11 K. At this temperature, the adsorbed oxygen partially remains in its molecular state.[6,7] The RDS intensities at 2.1 eV and 4.1 eV are completely quenched, which implies a strong interaction between the oxygen adsorbates and the surface state electrons. On the other hand, the features around 2.2 eV and 4.3 eV are much less affected, because of their bulk related origin. Besides the quenching of the surface state related signals, no new characteristic feature is induced at this stage. This suggests that the oxygen adsorbed on the Cu(110) surface does not yet induce a well ordered surface reconstruction. The LEED results are in support of this argument, showing only a blurred $p(1\times1)$ diffraction pattern with an increased diffuse background. A disordered adlayer is also expected considering the limited (if not fully frozen) mobility of the oxygen adsorbates at such a low temperature.

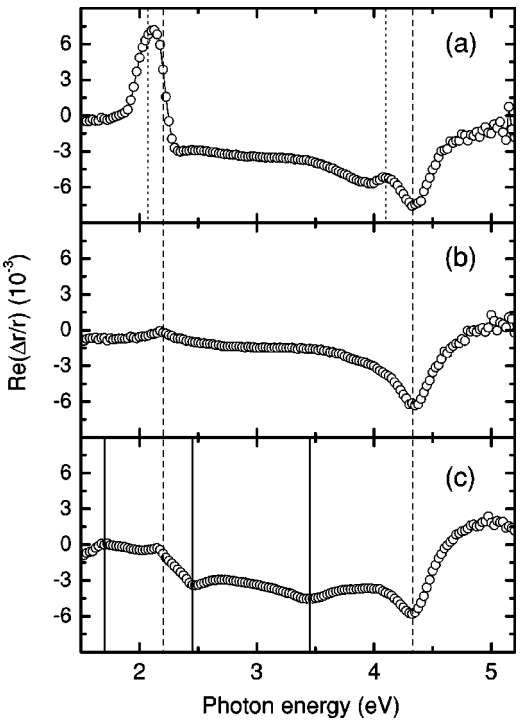

FIG. 1. Real part of the RDS spectrum recorded at 11 K from the clean Cu(110) surface (a), after adsorption of 1 L of oxygen at 11 K (b), and after heating to 550 K and cooling down to 11 K (c). The energy positions corresponding to surface state and bulk state related transitions of Cu(110) and to oxygen-induced transitions on Cu(110)-$c(6\times2)$O are marked by dotted, dashed, and solid vertical lines, respectively.

After annealing the sample to 550 K, a $c(6\times2)$ LEED pattern with sharp spots is observed [Fig. 2(b)]. Using the peak-to-peak ratio of the O_{KLL} and Cu_{LMM} Auger lines recorded from the fully developed (2×1)O surface as a reference for an oxygen coverage of $\Theta = 1/2$, the oxygen coverage corresponding to this sharp $c(6\times2)$ LEED pattern is determined to be $\Theta = 2/3$. These results indicate the formation of the Cu(110)-$c(6\times2)$O reconstructed phase with a surface structure proposed by Feidenhans'l *et al.*[2] Simultaneously, the RDS spectrum [Fig. 1(c)] reveals several well resolved new features, namely, a peak at 1.7 eV and two negative peaks at 2.5 eV and 3.5 eV. The peak at 1.7 eV is most probably contributed by optical transitions between new surface states induced by oxygen, since the energy is much lower than the onset of the *d*-band transition of bulk copper. The origin of the two oxygen induced negative peaks is not completely clear. Nevertheless, they can be used as a fingerprint of the $c(6\times2)$O phase.

B. Quantitative study of the $c(6\times2)$O→(2×1)O phase transition

In order to study the $c(6\times2)$O→(2×1)O phase transition at high temperature, the sample exhibiting a fully developed $c(6\times2)$O phase was repeatedly annealed using a con-

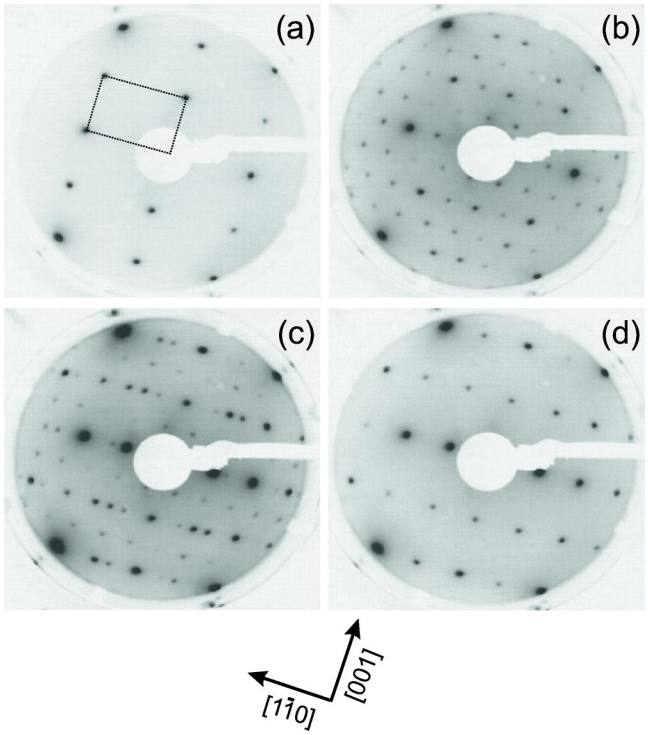

FIG. 2. LEED patterns recorded from the clean Cu(110) surface (a), after adsorption of 1 L of oxygen and subsequent annealing to 550 K (b), after three successive annealing cycles to 700 K (c), and after five annealing cycles to 700 K (d). Each annealing step consists of heating the surface to 700 K at a rate of 1 K/s and subsequent cooling down to 11 K as in the RDS experiments (Fig. 3). The unit cell of the bare (unreconstructed) Cu(110) surface is indicated in (a).

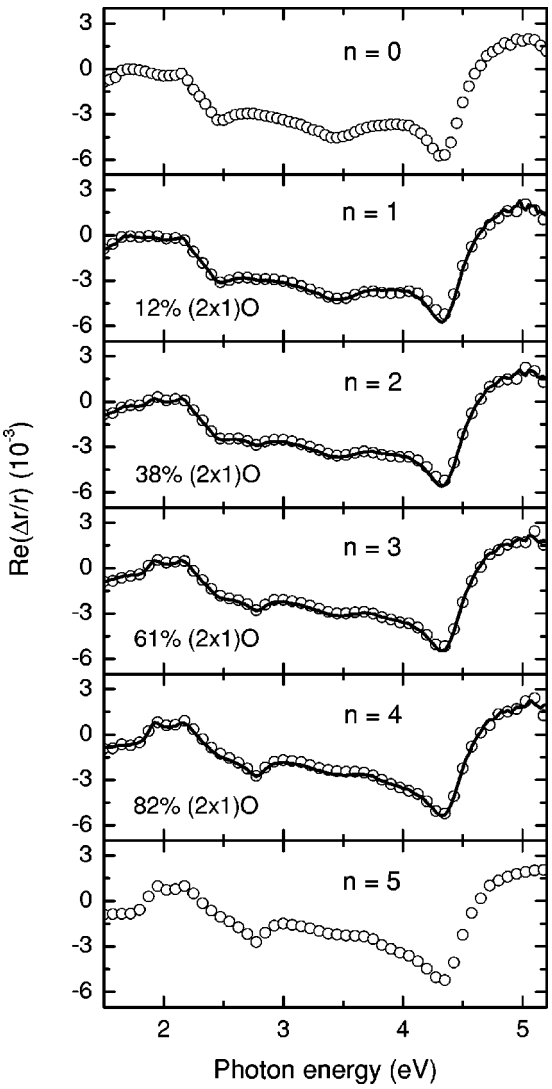

FIG. 3. Real part of the RDS spectra recorded after each annealing step $n=1,\ldots,5$, as indicated in the graphs. Open circles are the experimental data points, the solid lines are fits obtained by linear superposition of the RDS spectra of the pure $c(6\times2)$O phase ($n=0$) and the pure (2×1)O phase ($n=5$). The values $\chi_{(2\times1)}(n)$ for the best fits are also given.

trolled annealing procedure: the sample is first heated up to 700 K at a constant rate of 1 K/s and then cooled down to 11 K again. RDS spectra recorded after each annealing cycle $n=1,2,\ldots$ are shown in Fig. 3. The $c(6\times2)$O related features at 1.7 eV, 2.5 eV, and 3.5 eV become less pronounced after each annealing step. Simultaneously, a peak at 1.9 eV and a dip at 2.7 eV develop gradually, both of which are well-known features of the Cu(110)-(2×1)O surface.[11] Eventually, after the fifth annealing cycle ($n=5$), all the features belonging to the $c(6\times2)$O have completely disappeared and the RDS spectrum has transformed to that characteristic of the pure (2×1)O phase. This phase is stable upon further annealing up to temperatures as high as 800 K. Our observations agree with the report of Gruzalski *et al.*[5] The gradual change of the RDS spectra in Fig. 3 thus reflects the phase transition from the $c(6\times2)$O to the (2×1)O phase, which can also be followed by LEED as shown in Fig. 2. In addition, the LEED patterns reveal a "mixture" of the $c(6\times2)$ and (2×1) diffraction spots for intermediate annealing stages [see, e.g., Fig. 2(c) for $n=3$]. This implies the presence of well ordered regions with different reconstructions. Therefore, after the nth annealing step, the surface can be described by a coexistence of $c(6\times2)$O and (2×1)O domains, with relative weights or fractional area coverages $\sigma_{c(6\times2)}(n)$ and $\sigma_{(2\times1)}(n)$. Considering the fact that the coexisting phases were obtained upon annealing and ordering at high temperature and that the LEED spots in Fig. 2 are quite sharp, the number of defect sites must be rather small. In fact, previous STM images[22] reveal large domains of both phases separated by sharp and straight domain walls and, hence, $\sigma_{c(6\times2)}(n)+\sigma_{(2\times1)}(n)\simeq1$.

We have measured the Auger spectra for O_{KLL} and Cu_{LMM} after each annealing step n. We observe no detectable changes of the line shapes upon decreasing the oxygen coverage with each annealing step. Consequently, the peak-to-peak ratio of the O_{KLL} and Cu_{LMM} Auger signals I_O/I_{Cu} after each annealing step n should give a direct measure of the relative abundance of the two coexisting oxygen phases. The corresponding fractional area coverages $\sigma_{c(6\times2)}(n)$ and $\sigma_{(2\times1)}(n)$ can be extracted from

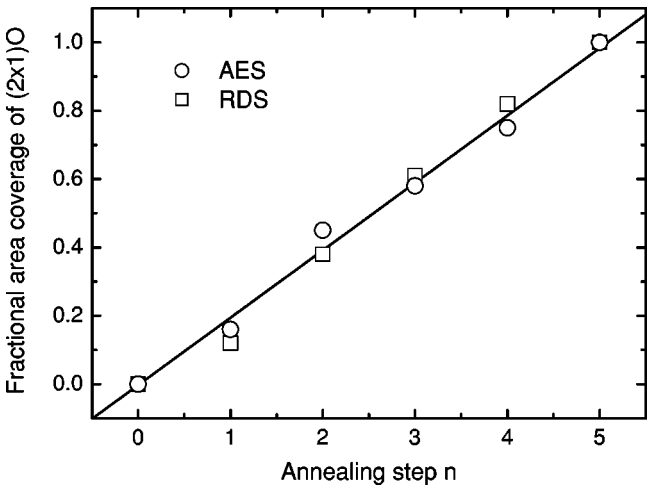

FIG. 4. Fractional area coverage of the (2×1)O phase after each annealing step (n) determined from AES [$\sigma_{(2\times1)}(n)$, open circles] and from the fits to the RDS spectra in Fig. 3 [$\chi_{(2\times1)}(n)$, open squares].

$$\frac{I_O}{I_{Cu}}(n)=\sigma_{(2\times1)}(n)\frac{I_O}{I_{Cu}}\bigg|_{(2\times1)}+\sigma_{c(6\times2)}(n)\frac{I_O}{I_{Cu}}\bigg|_{c(6\times2)}, \tag{2}$$

where $I_O/I_{Cu}|_{(2\times1)}$ and $I_O/I_{Cu}|_{c(6\times2)}$ are the Auger ratios corresponding to the pure $c(6\times2)$O and (2×1)O phases, respectively. Using $\sigma_{c(6\times2)}(n)=1-\sigma_{(2\times1)}(n)$, the so determined fractional area coverage $\sigma_{(2\times1)}(n)$ is plotted in Fig. 4 as open circles. Note that $\sigma_{(2\times1)}(n)$ varies almost linearly with the number of annealing steps, as will be discussed further below.

We will now demonstrate that the RDS spectra in Fig. 3 can be reproduced by the linear superposition of the RDS spectra of the pure (2×1)O and $c(6\times2)$O phases, in a similar way as the Auger peak-to-peak ratios in Eq. (2):

$$\frac{\Delta r}{r}(n)=\chi_{(2\times1)}(n)\frac{\Delta r}{r}\bigg|_{(2\times1)}+\chi_{c(6\times2)}(n)\frac{\Delta r}{r}\bigg|_{c(6\times2)}. \tag{3}$$

Here $\Delta r/r(n)$ represents the RDS spectrum after the nth annealing step, while $\Delta r/r|_{(2\times1)}$ and $\Delta r/r|_{c(6\times2)}$ are the characteristic RDS spectra of the pure (2×1)O and $c(6\times2)$O phase, respectively. $\chi_{(2\times1)}(n)$ and $\chi_{c(6\times2)}(n)=1-\chi_{(2\times1)}(n)$ denote the fractional area coverages of the (2×1)O and the $c(6\times2)$O phase after the nth annealing cycle. The solid lines in Fig. 3 show the best fits using $\chi_{(2\times1)}(n)$ as a free parameter. The fits are very good over the entire photon energy range of our measurement, and all the details of the spectra are well reproduced. The only slight but systematic deviation occurs around the RDS feature at 4.3 eV. This feature, related to a Cu optical transition, is known to be quite sensitive to surface electronic changes and strain.[21] We believe that the deviation arises from the local strain field in the vicinity of oxygen defect sites, namely the domain boundaries separating neighboring $c(6\times2)$O and (2×1) O domains.

The values of $\chi_{(2\times1)}(n)$ obtained from the fits to the RDS spectra in Fig. 3 are plotted as open squares in Fig. 4, again showing a linear increase with the number of annealing cycles. Most importantly, the values for $\chi_{(2\times1)(n)}$ are *identical* to those of $\sigma_{(2\times1)}(n)$ within experimental error, i.e., the same as those determined by AES. This result clearly shows that the optical anisotropy of this multidomain surface is the sum of those contributed from each of these domains. In fact, on semiconductor surfaces such as GaAs(113), it has been shown that the contribution of different reconstruction domains to the overall RDS spectrum is additive.[23,24] However, it is a bit surprising to see this analogy on Cu(110), since the additive property of the RDS spectrum on a semiconductor surface is based on the fact that all the electronic states are rather localized and insensitive to the size and shape of the corresponding domains. On metal surfaces like Cu(110), however, the free electronlike surface states are extended Bloch waves. Hence, the domain size and the total length of the domain boundaries may influence the RDS spectrum considerably.[18] A simple ''additive rule'' for coexisting domains is, thus, not expected for this type of states. On the other hand, one should keep in mind that the Cu(110) surface under consideration is fully covered by the oxygen-induced reconstruction domains, and the RDS features contributed by the intrinsic free electronlike states on Cu(110) have already been quenched upon oxygen adsorption. The remaining RDS spectrum contains only the transitions involving surface modified *d*-band electrons and oxygen derived surface states. Since both of these are rather localized states and because the domains are extended and well ordered giving rise to sharp LEED patterns (Fig. 2), it becomes reasonable to extend the additive rule to the present case. With the help of this additive rule, quantitative information such as the oxygen coverage and the relative population of the different reconstruction phases can be readily extracted from a single RDS spectrum. Furthermore, since the variation of the RDS signal at any energy during annealing is proportional to the change of the oxygen coverage, phase transitions such as $c(6\times2)$O$\rightarrow(2\times1)$O can be followed by monitoring the RDS signal at the most suitable, characteristic photon energy.

The *linear* variation of the fractional area coverages with the number of annealing cycles indicates that the oxygen removal is *independent* of the $c(6\times2)$O coverage prior to the nth annealing step. In other words, the oxygen removal rate $-d\Theta/dt$ (at a given temperature) is independent of the oxygen coverage Θ, suggesting zero-order kinetics during the transition from the $c(6\times2)$O to the (2×1)O phase. In fact, the STM images in Ref. 22 show that both $c(6\times2)$O and (2×1)O domains are stripelike with the domain boundaries running along the [001] direction when they coexist on the surface. If one assumes that the oxygen removal only occurs at the linear [one-dimensional (1D)] domain boundaries between (2×1)O and $c(6\times2)$O domains, whose density remains essentially constant during the phase transition, then a zero-order behavior is, indeed, expected. In this case, the fractional area of the (2×1)O domains should grow at a constant rate [at the expense of the $c(6\times2)$O stripes] by the movement of the 1D domain boundaries.

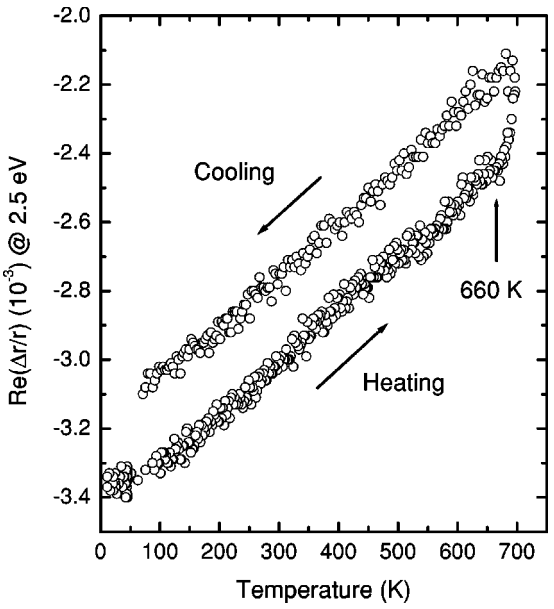

FIG. 5. RDS intensity recorded at a fixed photon energy of 2.5 eV during the first annealing cycle to 700 K.

C. Real-time study of the $c(6\times2)$O→(2×1)O phase transition

By following the RDS signal at a fixed photon energy as a function of time (so called ''kinetic'' or RDK measurements), the phase transition has been monitored during each annealing cycle in real time. As an example, the RDS signal recorded for a photon energy of 2.5 eV during the first annealing cycle is shown in Fig. 5. The linear increase of the signal (decrease of the absolute anisotropy) of the signal between 11 K and 660 K during heating can be ascribed to a temperature effect. This is confirmed by the observation of the same slope during cooling down. In contrast, the increase between 660 K and 700 K is much faster and corresponds to the partial transformation of the $c(6\times2)$O domains into the (2×1)O phase due to the decrease of the oxygen surface coverage. Based on the RDK spectra, we conclude that 660 K is the onset temperature for the $c(6\times2)$O→(2×1)O phase transition. Gruzalski *et al.*[5] have observed the same phase transition with LEED and X-ray photoelectron spectroscopy (XPS), reporting an onset temperature of 610 K, which is lower than the 660 K inferred from the RDK results. The lower onset temperature could be due to the different annealing procedure performed in their study (5 min staying at the specified temperature). Their argument, that the oxygen lost during the phase transition has diffused into the copper bulk, is supported by the fact that no oxygen desorption has been reported up to now. Nevertheless, some of our experimental results indicated that the amount of oxygen removed from the surface is probably also related to subsurface defects or impurities such as carbon on the Cu(110) surface. Further investigations are presently underway to gain a better understanding of the oxygen removal mechanism.

IV. CONCLUSION

Adsorption of 1 L of oxygen on Cu(110) at 11 K quenches all the anisotropy arising from the optical transitions involving metal surface states and leaves only the contribution of the surface modified *d*-band transitions. Heating the oxygen covered Cu(110) surface up to 550 K induces a fully developed $c(6\times2)$O reconstruction with an oxygen coverage $\Theta = 2/3$. Further annealing to temperatures higher than 660 K leads to a phase transition from the $c(6\times2)$O to the (2×1)O phase. The contribution of different reconstructed domains to the RDS spectrum during this phase transition is additive. As a result, the oxygen coverage and the fractional area coverage of the different reconstructions can be extracted directly from the RDS spectrum. By monitoring the RDS intensity at a photon energy of 2.5 eV during annealing, the onset temperature of the phase transition has been determined to be 660 K.

ACKNOWLEDGMENTS

This work was financially supported by the Austrian Science Fund (FWF) under contract No. 15963-N08. We also would like to acknowledge fruitful discussions with R. E. Balderas-Navarro.

*Electronic address: zeppenfeld@exphys.uni-linz.ac.at

[1] F. Besenbacher and J.K. Nørskov, Prog. Surf. Sci. **44**, 5 (1993).
[2] R. Feidenhans'l, F. Grey, M. Nielsen, F. Besenbacher, F. Jensen, E. Lægsgaard, I. Stensgaard, K.W. Jacobsen, J.K. Nørskov, and R.L. Johnson, Phys. Rev. Lett. **65**, 2027 (1990).
[3] W. Liu, K.C. Wong, and K.A.R. Mitchell, Surf. Sci. **339**, 151 (1995).
[4] G.R. Gruzalski, D.M. Zehner, and J.F. Wendelken, Surf. Sci. **147**, L623 (1984).
[5] G.R. Gruzalski, D.M. Zehner, J.F. Wendelken, and R.S. Hathcock, Surf. Sci. **151**, 430 (1985).
[6] B.G. Briner, M. Doering, H.-P. Rust, and A.M. Bradshaw, Phys. Rev. Lett. **78**, 1516 (1997).
[7] A. Hodgson, A.K. Lewin, and A. Nesbitt, Surf. Sci. **293**, 211 (1993).
[8] D.E. Aspnes, J. Vac. Sci. Technol. B **3**, 1498 (1985).
[9] D.S. Martin and P. Weightman, Surf. Interface Anal. **31**, 915 (2001).
[10] Ph. Hofmann, K.C. Rose, V. Fernandez, A.M. Bradshaw, and W. Richter, Phys. Rev. Lett. **75**, 2039 (1995).
[11] K. Stahrenberg, Th. Herrmann, N. Esser, and W. Richter, Phys. Rev. B **61**, 3043 (2000).
[12] J. Bremer, J.-K. Hansen, and O. Hunderi, Appl. Surf. Sci. **142**, 286 (1999).
[13] Y. Borensztein, W.L. Mochan, J. Tarriba, R.G. Barrera, and A. Tadjeddine, Phys. Rev. Lett. **71**, 2334 (1993).
[14] J.-K. Hansen, J. Bremer, and O. Hunderi, Surf. Sci. **418**, L58 (1998).
[15] K. Stahrenberg, Th. Herrmann, N. Esser, J. Sahm, W. Richter, S.V. Hoffmann, and Ph. Hofmann, Phys. Rev. B **58**, R10 207 (1998).
[16] B. Sheridan, D.S. Martin, J.R. Power, S.D. Barrett, C.I. Smith,

C.A. Lucas, R.J. Nichols, and P. Weightman, Phys. Rev. Lett. **85**, 4618 (2000).
[17] V. Mazine and Y. Borensztein, Phys. Rev. Lett. **88**, 147403 (2002).
[18] L.D. Sun, M. Hohage, P. Zeppenfeld, R.E. Balderas-Navarro, and K. Hingerl, Phys. Rev. Lett. **90**, 106104 (2003).
[19] J. Bremer, J.K. Hansen, and O. Hunderi, Surf. Sci. **436**, L735 (1999).
[20] D.E. Aspnes, J.P. Harbison, A.A. Studna, and L.T. Florez, J. Vac. Sci. Technol. A **6**, 1327 (1988).
[21] L.D. Sun, M. Hohage, P. Zeppenfeld, R.E. Balderas-Navarro, and K. Hingerl, Surf. Sci. **527**, L184 (2003).
[22] D. Coulman, J. Wintterlin, J.V. Barth, and G. Ertl, Surf. Sci. **240**, 151 (1990).
[23] M. Pristovsek, H. Menhal, T. Wehnert, J.-T. Zettler, T. Schmidtling, N. Esser, W. Richter, C. Setzer, J. Platen, and K. Jacobi, J. Cryst. Growth **195**, 1 (1998).
[24] J.-T. Zettler, J. Rumberg, K. Ploska, K. Stahrenberg, M. Pristovsek, W. Richter, M. Wassermeier, P. Schützendüwe, J. Behrend, and L. Däweritz, Phys. Status Solidi A **152**, 35 (1995).